

DEUTSCHES ELEKTRONEN-SYNCHROTRON **DESY**

DESY 85-022
February 1985

A SEARCH FOR MONOJET EVENTS PRODUCED BY VIRTUAL Z^0 BOSONS
IN e^+e^- ANNIHILATION AT PETRA

by

JADE Collaboration

ISSN 0418-9833

NOTKESTRASSE 85 · 2 HAMBURG 52

DESY behält sich alle Rechte für den Fall der Schutzrechtserteilung und für die wirtschaftliche Verwertung der in diesem Bericht enthaltenen Informationen vor.

DESY reserves all rights for commercial use of information included in this report, especially in case of filing application for or grant of patents.

To be sure that your preprints are promptly included in the
HIGH ENERGY PHYSICS INDEX ,
send them to the following address (if possible by air mail) :

DESY
Bibliothek
Notkestrasse 85
2 Hamburg 52
Germany

A SEARCH FOR MONOJET EVENTS PRODUCED BY VIRTUAL Z^0 BOSONS
IN e^+e^- ANNIHILATION AT PETRA

JADE Collaboration

W. Bartel, L. Becker, D. Cords¹, R. Felst, K. Hagiwara, D. Haidt, H. Junge²,
G. Knies., H. Krehbiel, P. Laurikainen³, R. Meinke, B. Naroska, J. Olsson,
D. Schmidt², P. Steffen
Deutsches Elektronen-Synchrotron DESY, Hamburg, Germany

G. Dietrich, J. Hagemann, G. Heinzemann, H. Kado, C. Kleinwort,
M. Kuhlen, K. Meier⁴, A. Petersen¹, R. Ramcke U. Schneekloth, G. Weber
II. Institut für Experimentalphysik der Universität Hamburg, Germany

K. Ambrus, S. Bethke, A. Dieckmann, E. Elsen, J. Heintze,
K.H. Hellenbrand, S. Komamiya, J. von Krogh, P. Lennert, H. Matsumura,
H. Rieseberg, J. Spitzer, A. Wagner
Physikalisches Institut der Universität Heidelberg, Germany

C. Bowdery, A. Finch, F. Foster, G. Hughes, T. Nozaki⁵, J. Nye
University of Lancaster, England

J. Allison, A.H. Ball, R.J. Barlow, J. Chrin, I.P. Duerdoth, T. Greenshaw,
P. Hill, F.K. Loebinger, A.A. Macbeth, H.E. Mills, P.G. Murphy, K. Stephens,
P. Warming
University of Manchester, England

R.G. Glasser, B. Sechi-Zorn⁶, J.A.J. Skard, S.R. Wagner, G.T. Zorn
University of Maryland, Maryland, USA

S.L. Cartwright, D. Clarke, R. Marshall, R. Middleton, J.B. Whittaker
Rutherford Appleton Laboratory, Chilton, England

T. Kawamoto, T. Kobayashi, T. Mashimo, M. Minowa, H. Takeda,
T. Takeshita, S. Yamada
ICEPP University of Tokyo, Japan

¹Now at SLAC, California, USA

²Universität-Gesamthochschule Wuppertal, Germany

³University of Helsinki, Helsinki, Finland

⁴Now at CERN, Geneva, Switzerland

⁵Now at KEK, Ibaraki, Japan

⁶Deceased

Abstract

A search was performed for the associated production of two different Higgs bosons via a virtual Z^0 in e^+e^- annihilation ($e^+e^- \rightarrow h_1^0 h_2^0$) using the JADE detector at PETRA. This was motivated by the interpretation of the monojet events observed at the CERN $p\bar{p}$ collider as anomalous Z^0 decays into two neutral Higgs bosons (h_1^0 and h_2^0), where h_1^0 is stable and escapes detection while h_2^0 decays into hadrons. Single- or di-jet events with large momentum imbalance are then expected at PETRA energies. No evidence for such events was found in our data; this excludes h_2^0 masses in the range of 1 to 21 GeV with 95% C.L., if the branching fraction for $Z^0 \rightarrow h_1^0 h_2^0$ is larger than one half that for $Z^0 \rightarrow \nu_\mu \bar{\nu}_\mu$. The possibility that the monojets could originate from supersymmetric higgsino production from Z^0 decay is also examined.

Recently, the UA1 collaboration at the CERN $p\bar{p}$ collider has reported the observation of monojet events. These are events characterised by a single, high transverse momentum jet and large missing transverse momentum ⁽¹⁾. It has been suggested that such events can be explained by the anomalous decay of the Z^0 into two neutral particles, one being long lived and escaping the detector, and the other one producing a jet through its decay products. One possibility is the decay of the Z^0 into two neutral Higgs bosons ⁽²⁾. Another explanation would be the supersymmetric alternative, namely the Z^0 decay into two neutral higgsinos ⁽³⁾⁽⁴⁾. All such models in which monojets arise from Z^0 decay have in common that they also predict the occurrence of monojet events in e^+e^- annihilation at high energies ⁽²⁾.

In this paper we compare the predictions of these models with the e^+e^- data taken with the JADE detector at PETRA and give mass limits for the particles proposed to explain the UA1 monojet events.

The decay of Z^0 into two different Higgs bosons (h_1^0 and h_2^0), within the framework of a model with two Higgs doublets, was proposed by Glashow and Manohar ⁽²⁾ as an explanation of the UA1 monojet events. Note that Bose statistics forbid Z^0 decay into a pair of identical spin zero particles. One of the produced Higgs bosons (h_1^0) would have to be light enough ($M(h_1^0) < 2M(\mu^\pm)$) in order to have a reasonably long lifetime, whilst the other (h_2^0) would decay into hadrons and produce a jet. To be consistent with the characteristics of the observed monojets, the heavier Higgs boson h_2^0 would need a mass of several GeV ⁽²⁾, and hence the dominant decay modes would be $h_2^0 \rightarrow c\bar{c}$ and $\tau\bar{\tau}$ (and $b\bar{b}$ if kinematically allowed).

The total and differential cross sections for the process $e^+e^- \rightarrow h_1^0 h_2^0$ mediated by a virtual Z^0 (Fig.1a) are given in Refs.3 and 5. The total cross section is ≈ 0.6 pb at $\sqrt{s} = 45$ GeV if h_1^0 and h_2^0 are sufficiently light. For a heavy h_2^0 , the total cross section is decreased by a factor β^3 , where β is the momentum of the Higgs bosons in the e^+e^- C.M. system divided by the beam energy. Since h_1^0 and h_2^0 are spin zero bosons, the angular distribution is proportional to $\sin^2\vartheta$, where ϑ denotes the polar angle. We assumed that h_1^0 is stable and h_2^0 decays either into fermion pairs $f\bar{f}$ (Fig.1b) or into $f\bar{f}h_1^0$ (Fig.1c). For the analysis we fixed the mass of the light Higgs at $M(h_1^0) = 0.2$ GeV and kept $M(h_2^0)$ free. The partial decay width of the $h_2^0 \rightarrow f\bar{f}$ mode is proportional to $N_c \cdot m_f^2 \cdot \beta_f^3$, where $N_c = 1$ for leptons and $N_c = 3$ for quarks, m_f is the fermion mass and β_f is the velocity of f in the h_2^0 rest frame. However, the absolute normalization of the partial width depends on the vacuum expectation values of the Higgs bosons which is unknown. The three body decay mode $h_2^0 \rightarrow h_1^0 f\bar{f}$ is mediated by a virtual Z^0 , as in the case of the production process $e^+e^- \rightarrow h_1^0 h_2^0$. Its partial width is hence proportional to the $Z^0 f\bar{f}$ coupling constant,

which is well known. Due to the unknown normalization in $\Gamma(h_2^0 \rightarrow f\bar{f})$, the two body decay branching fraction

$$r = \frac{\sum \Gamma(h_2^0 \rightarrow f\bar{f})}{[\sum \Gamma(h_2^0 \rightarrow f\bar{f}) + \sum \Gamma(h_2^0 \rightarrow h_1^0 f\bar{f})]}$$

is arbitrary and chosen as a free parameter in our analysis.

The production and decay processes were simulated by a Monte Carlo event generator using the differential cross section and decay matrix elements given in Ref.3. For the hadronic fragmentation of the $q\bar{q}$ system, the Lund model was used ⁽⁶⁾. The parameters in the Lund model were optimized to the multihadron data ⁽⁷⁾, especially the charged multiplicity. Detector effects were fully simulated in the Monte Carlo. In order to calculate the detection efficiency, the Monte Carlo data were passed through the same analysis chain which was applied to the real data.

The data analysis was based on an integrated luminosity of 74 pb^{-1} for the C.M. energy range 27.00-37.00 GeV and 20 pb^{-1} for the C.M. energy range 38.00-46.78 GeV. The details of the JADE detector and the trigger conditions have been described elsewhere ⁽⁸⁾.

The selection criteria for the $e^+e^- \rightarrow h_1^0 h_2^0$ events were similar to those used previously in our search for single zino production associated with a photino ($e^+e^- \rightarrow Z\tilde{\gamma}$), where the zino decays into $q\bar{q}\tilde{\gamma}$ or $q\bar{q}\tilde{g}$ ⁽⁹⁾. Similar to the zino case, a heavy h_2^0 ($M(h_2^0) \gtrsim \sqrt{s}/2$) will appear as an acoplanar two jet event rather than a monojet. For a light h_2^0 ($M(h_2^0) \lesssim \sqrt{s}/2$), the hadrons from the h_2^0 decay form a monojet. We have studied both these cases using the standard multihadron event sample. For h_2^0 masses below 2 GeV the multiplicity of the monojet would be too low for the events to be contained in the multihadron event sample. For this case a special low multiplicity event sample was investigated.

We started the event selection from the multihadron data sample; the selection criteria for this sample have been described elsewhere ⁽¹⁰⁾. We applied all the cuts in Ref.10, except for the visible energy cut and the longitudinal momentum balance requirement (cuts (8) and (9), respectively, in Ref.10). The essential requirement is that at least four charged particles come from the event vertex.

The monojet events were selected by the following criteria:

- (A1) The polar angle of the event thrust direction had to satisfy $|\cos\vartheta_{th}| < 0.65$, where ϑ_{th} is the polar angle of the event thrust axis relative to the positron beam direction.
- (A2) The missing transverse momentum P_{Tmiss} relative to the beam had to exceed 7 GeV.

- (A3) The plane normal to the thrust axis defines two hemispheres. The total visible energy E_{back} of all the particles in the backward hemisphere, i.e. opposite to the thrust axis, was required to be small: $E_{\text{back}} < 1 \text{ GeV}$.
- (A4) In order to reject $\tau^+\tau^-$ events with very acoplanar charged tracks, no charged tracks were allowed at all in the backward hemisphere, in addition to the cut (A3).
- (A5) Cuts (A1) to (A4) can be satisfied by events with an energetic photon escaping through a gap between the leadglass blocks thus causing a high P_{Tmiss} . To avoid such contributions the following additional requirements were added:
 - Events were rejected if the innermost barrel muon chamber exhibited hits within $\pm 10^\circ$ of the missing transverse momentum direction which were consistent with hits due to an electromagnetic shower.
 - Events were rejected if the forward muon chambers behind the gap between the barrel and endcap leadglass counters showed hits.
 - Runs with the muon chambers not in operation were rejected and the corresponding integrated luminosity was subtracted in the calculations of the limits.

The scatter plot of E_{back} versus P_{Tmiss} , for the data with $\sqrt{s} > 38 \text{ GeV}$, is shown in Fig.2a, after applying the cut (A1). The cuts (A2) and (A3) are indicated in the figure. The cuts (A4) and (A5) are not necessary for the data with $\sqrt{s} > 38 \text{ GeV}$, as is shown in Fig.2a. For the data with $27 < \sqrt{s} < 37 \text{ GeV}$, an equivalent plot has been given in Ref.9 (see Fig.3(a) in that paper). No events survived after all the above cuts. Figure 2b shows the prediction for $e^+e^- \rightarrow h_1^0 h_2^0$ events, with the subsequent decay $h_2^0 \rightarrow f\bar{f}$, for $M(h_1^0) = 0.2 \text{ GeV}$ and $M(h_2^0) = 8 \text{ GeV}$. Most of the h_2^0 bosons decay into $c\bar{c}$ or $\tau\bar{\tau}$ in this case. The detection efficiency for this case is about 75 % at $M(h_2^0) = 5 \text{ GeV}$. It stays almost constant up to about $M(h_2^0) = 10 \text{ GeV}$, and decreases to 15 % when $M(h_2^0)$ is increased to 20 GeV. For $M(h_2^0)$ below 2 GeV, the detection efficiency is limited by the charged multiplicity cut, and falls sharply with decreasing $M(h_2^0)$. For the $h_2^0 \rightarrow h_1^0 f\bar{f}$ decay, the detection efficiency is about a factor of two smaller than for the previous case at $M(h_2^0) = 5 \text{ GeV}$. The two detection efficiencies are almost identical at $M(h_2^0) = 15 \text{ GeV}$.

The selection criteria for the events with acoplanar jets were the following:

- (B1) The visible energy of the event E_{vis} was required to satisfy

$(2/5)\sqrt{s} < E_{\text{vis}} < \sqrt{s}$, where E_{vis} was obtained by summing the momenta of the charged tracks and the energies of the leadglass clusters.

- (B2) The polar angle ϑ_{th} of the event thrust axis had to satisfy $|\cos\vartheta_{\text{th}}| < 0.65$.
- (B3) Two hemispheres were defined by the plane perpendicular to the thrust axis. In each hemisphere the particle momenta were summed vectorially. With the two resultant momenta (\vec{p}_1 and \vec{p}_2) the acoplanarity angle φ_{acop} between the plane defined by \vec{p}_1 and the beam direction and the plane defined by \vec{p}_2 and the beam direction was calculated: $\cos\varphi_{\text{acop}} = -(\vec{p}_1 \times \hat{z}) \cdot (\vec{p}_2 \times \hat{z}) / (|\vec{p}_1 \times \hat{z}| |\vec{p}_2 \times \hat{z}|)$ where \hat{z} denotes a unit vector in the positron beam direction. Only events with large acoplanarity were selected:
 $\varphi_{\text{acop}} > 40^\circ \cdot (1 + |\cos\vartheta_{\text{th}}|)$
- (B4) Remaining very acoplanar $\tau^+\tau^-$ events were rejected by the requirement that the number of charged tracks found in each thrust hemisphere was not equal to one.

The scatter plot of $|\cos\vartheta_{\text{th}}|$ versus φ_{acop} is shown in Fig.3a for those events with $\sqrt{s} > 38 \text{ GeV}$ which satisfy the cut (B1). The cuts (B2) and (B3) are indicated in the figure. For the data taken with C.M. energy between 27 GeV and 37 GeV, the equivalent plot has been given in Ref.9 (see Fig3(b) in that paper), with a softer E_{vis} cut ($(1/3)\sqrt{s} < E_{\text{vis}} < \sqrt{s}$) applied. Again no event survived after all the cuts. The distribution expected, for $e^+e^- \rightarrow h_1^0 h_2^0$ with $M(h_1^0) = 0.2 \text{ GeV}$ and $M(h_2^0) = 20 \text{ GeV}$ is shown in Fig.3b. The detection efficiency for the $h_2^0 \rightarrow f\bar{f}$ decay is about 60 % at $M(h_2^0) = 5 \text{ GeV}$ and decreases slowly to 40 % with $M(h_2^0)$ increasing to 20 GeV. For $M(h_2^0)$ smaller than 2 GeV the efficiency decreases very rapidly due to the charged multiplicity cut of four. In the case of the $h_2^0 \rightarrow h_1^0 f\bar{f}$ decay, the efficiency is lower but approaches the $h_2^0 \rightarrow f\bar{f}$ efficiency for large h_2^0 masses ($\gtrsim 15 \text{ GeV}$).

The search for monojets for the case of very light Higgs masses was made in a special two prong event sample. This sample contained events with two oppositely charged particles coming from the fiducial cylinder of radius 20 mm and length $\pm 200 \text{ mm}$ along z and having momenta greater than 0.2 GeV. There was no restriction on the number of photons but the total energy deposit in the barrel leadglass counters had to be larger than 3 GeV. To select monojet events the following cuts were applied:

- (C1) All particle momenta were summed vectorially. The polar angle ϑ_{tot} of the resultant momentum \vec{P}_{tot} had to satisfy $|\cos\vartheta_{\text{tot}}| < 0.65$.

- (C2) The total missing transverse momentum ($|\vec{P}_{\text{tot}}| \cdot |\sin\vartheta_{\text{tot}}|$) had to be larger than 7 GeV.
- (C3) The total leadglass cluster energy outside a cone around the \vec{P}_{tot} direction with an opening angle of 60° had to be smaller than 0.2 GeV.
- (C4) No charged particle with momentum larger than 0.08 GeV was allowed outside the cone.
- (C5) The energy deposit in the forward tagging counters was required to be smaller than 1 GeV in order to reject $e^+e^- \rightarrow e^+e^-e^+e^-$ events from the two photon process.

Of a total of 887,000 events in the two prong sample, no events survived the above cuts. The detection efficiency for the $h_2^0 \rightarrow f\bar{f}$ decay was calculated to vary from 10 % to 15 % for $M(h_2^0)$ in the range 0.7 to 3 GeV.

For the h_2^0 mass limit calculation the results from selections A, B and C were combined. Since the samples selected by the cuts (A1)-(A5) and by (B1)-(B4) are partially overlapping, the event selection (A or B) yielding the higher efficiency was taken in the combination. The detection efficiency for the $h_2^0 \rightarrow f\bar{f}$ case (ε) and that for the $h_2^0 \rightarrow h_1^0 f\bar{f}$ case (ε') were calculated separately for a given $M(h_2^0)$. The losses due to unseen non-hadronic decay modes are taken into account in ε and ε' . The efficiencies were determined from a Monte Carlo event sample generated with the theoretical cross section within the range of C.M. energies considered, by taking into account the experimental luminosity as a function of energy. The total number of events expected for a given $M(h_2^0)$ is $N_{\text{exp}} = N_{\text{prod}}[\varepsilon \cdot r + \varepsilon'(1-r)]$, where N_{prod} denotes the total number of events expected from the theoretical cross section in the C.M. energy range considered. Here r is the branching fraction of the $h_2^0 \rightarrow f\bar{f}$ decay summed over all possible fermion pairs, as defined above. By comparing the theoretically expected number with the 95 % C.L. limit, which is three events since zero events were observed, the excluded region in the r - $M(h_2^0)$ plane was obtained. This is shown in Fig.4a. The Higgs boson h_2^0 can be excluded in the mass range from less than 1 GeV to 21 GeV, almost independently of the branching fraction r .

The above results are valid in the framework of the Glashow-Manohar model. To make a more model independent analysis, we allowed the coupling constant of the $Z^0 h_1^0 h_2^0$ vertex, which is fixed in the Glashow-Manohar model, to be free. Thus the ratio $\xi = \Gamma(Z^0 \rightarrow h_1^0 h_2^0) / \Gamma(Z^0 \rightarrow \nu_\mu \bar{\nu}_\mu)$ was chosen as a free parameter so that our limit can be more generally compared with results from the $p\bar{p}$ collider. In the Glashow-Manohar model ξ is equal to $\beta^3/2$, where β is the momentum of

the Higgs bosons in the Z^0 rest frame divided by $M(Z^0)/2$. For $M(h_2^0) \ll M(Z^0)$, β is close to one. In this general case the total cross section of $e^+e^- \rightarrow h_1^0 h_2^0$ via virtual Z^0 is given by $\xi \cdot (\beta^3/\beta^3) \cdot \sigma(e^+e^- \rightarrow \nu_\mu \bar{\nu}_\mu)$, where β has been defined previously (the momentum of Higgs bosons in the e^+e^- C.M. system divided by the beam energy). The number of events expected was calculated as a function of ξ , r and $M(h_2^0)$ while $M(h_1^0)$ was fixed to 0.2 GeV, as before. The excluded region in the ξ - $M(h_2^0)$ plane is shown in Fig.4b for various values of r . For ξ larger than 0.5 the upper and lower experimental mass limits are 1 GeV and 21 GeV, respectively, independent of r . A reduction of $M(h_1^0)$ from 0.2 GeV to zero results in slightly better limits only in the $M(h_2^0)$ mass region below 2 GeV.

An alternative explanation of the UA1 monojet events is the supersymmetric version of the previous models. Monojet events may arise from Z^0 decay into different higgsinos $Z^0 \rightarrow \tilde{\chi}_1^0 \tilde{\chi}_2^0$ (Fig.1d). One of the higgsinos $\tilde{\chi}_1^0$ would be light and stable whereas the other one $\tilde{\chi}_2^0$ would decay into $\tilde{\chi}_1^0 f\bar{f}$ (Fig.1e) ⁽³⁾. In the analysis we assumed a massless $\tilde{\chi}_1^0$. In general, the higgsinos can be mixed with each others and with photinos and zinos ⁽¹¹⁾. For definiteness and simplicity we consider here only the case of pure higgsino mixing. Since the vacuum expectation values for Higgs fields and their mixing angles are unknown, the coupling constant at the $Z^0 \tilde{\chi}_1^0 \tilde{\chi}_2^0$ vertex is not known. For this reason the ratio $\xi = \Gamma(Z^0 \rightarrow \tilde{\chi}_1^0 \tilde{\chi}_2^0) / \Gamma(Z^0 \rightarrow \nu_\mu \bar{\nu}_\mu)$ was chosen as a free pararameter in the analysis. The production and decay processes were again simulated by a Monte Carlo event generator using the differential cross section and decay matrix elements given in Ref.3. The detection efficiencies with the A, B or C selection criteria are about the same as those for the case $h_2^0 \rightarrow h_1^0 f\bar{f}$ at the same mass. In Fig.4c, the excluded region in ξ - $M(\tilde{\chi}_2^0)$ plane is shown. If ξ is larger than 0.5, the excluded region for $M(\tilde{\chi}_2^0)$ with 95% C.L. is from 1.3 GeV to 24.7 GeV. At large masses the limit is slightly better than that for $e^+e^- \rightarrow h_1^0 h_2^0$ with $r = 0$ because suppression due to the threshold effect is weaker. For small masses the limit is slightly worse because of the different angular distribution. The ratio ξ is a function of the higgsino mixing angle(s). Within two doublet models ⁽⁴⁾ ξ is limited to values smaller than 2. This upper bound, which is valid for maximum mixing, is also given in Fig.4c.

In summary, no evidence for monojets produced by virtual Z^0 bosons was found in our data. The Glashow-Manohar interpretation of the UA1 monojet events as anomalous Z^0 decays into two different Higgs bosons has been excluded if the mass of the heavier Higgs boson lies between 1 and 21 GeV. Similar mass limits were obtained for the case of Z^0 decay into two neutral higgsinos.

Acknowledgement

We are indebted to the PETRA machine group for their excellent support and to all the engineers and technicians who have participated in the construction and maintenance of the apparatus. This experiment was supported by the Bundesministerium für Forschung und Technologie, by the Japanese Ministry of Education, Science and Culture, by the UK Science and Engineering Research Council through the Rutherford Appleton Laboratory, and the U.S. Department of Energy. The visiting groups wish to thank the DESY directorate for the hospitality extended to them.

REFERENCES

- 1) UA1 Collaboration, G. Arnison et al., Phys. Lett. 139B(1984)115
- 2) S.L. Glashow and A. Manohar, Phys. Rev. Lett. 54(1985)528
- 3) H. Bare, K. Hagiwara and S. Komamiya, DESY 85-012, submitted to Phys. Lett.
- 4) J. Ellis, J.S. Hagelin, D.V. Nanopoulos and M. Srednicki, Phys. Lett. 127B(1983)233
J. Ellis, J.-M. Frère, J.S. Hagelin, G.L. Kane and S.T. Petcov, Phys. Lett. 132B(1983)436
- 5) G. Poćik and G. Zsigmond, Z. Physik C10(1981)367
- 6) B. Anderson, G. Gustafson G. Ingelman and T. Sjöstrand, Physics Reports 97(1983)33
T. Sjöstrand, Computer Phys. Comm. 27(1982)243
- 7) JADE- Collaboration, W. Bartel et al., Z. Physik C20(1983)187
- 8) JADE- Collaboration, W. Bartel et al., Phys. Lett. 88B(1979)171
- 9) JADE- Collaboration, W. Bartel et al., Phys. Lett. 146B(1984)126
- 10) JADE- Collaboration, W. Bartel et al., Phys. Lett. 129B(1983)145
- 11) K. Inoue, A. Kakuto, H. Komatsu and S. Takeshita, Prog. Theor. Phys. 67(1982)1889
J. Ellis and G.G. Ross, Phys. Lett. 117B(1982)397

FIGURE CAPTIONS

FIG. 1 Diagrams for Higgs/higgsino production and decay

- (a) Associated production of nonminimal Higgs bosons h_1^0 and h_2^0 via a virtual Z^0 in e^+e^- annihilation
- (b) Decay of h_2^0 into a fermion pair
- (c) Decay of h_2^0 into a fermion pair plus h_1^0
- (d) Associated production of higgsinos $\tilde{\chi}_1^0$ and $\tilde{\chi}_2^0$ via a virtual Z^0 in e^+e^- annihilation
- (e) Decay of $\tilde{\chi}_2^0$ into a fermion pair plus $\tilde{\chi}_1^0$

FIG. 2 (a) Scatter plot of E_{back} versus P_{miss} for the events ($\sqrt{s} > 38$ GeV) passing cut (A1). The cuts (A2) and (A3) are indicated by full lines.

(b) The same plot for the Monte Carlo generated events $e^+e^- \rightarrow h_1^0 h_2^0$ with $M(h_1^0) = 0.2$ GeV, $h_2^0 = 8$ GeV for the decay $h_2^0 \rightarrow f\bar{f}$.

FIG. 3 (a) Scatter plot $|\cos\theta_{\text{th}}|$ versus acoplanarity angle for the events ($\sqrt{s} > 38$ GeV) passing cut (B1). The final cuts are indicated by full lines.

(b) The same plot for the Monte Carlo generated events $e^+e^- \rightarrow h_1^0 h_2^0$ with $M(h_1^0) = 0.2$ GeV, $M(h_2^0) = 20$ GeV for the decay $h_2^0 \rightarrow f\bar{f}$.

FIG. 4 (a) Excluded region in the $r - M(h_2^0)$ plane with 95% C.L., where $r = \sum \Gamma(h_2^0 \rightarrow f\bar{f}) / [\sum \Gamma(h_2^0 \rightarrow f\bar{f}) + \sum \Gamma(h_2^0 \rightarrow h_1^0 f\bar{f})]$.

(b) Excluded region in the $M(h_2^0) - \xi$ plane for $r = 0$, $r=0.5$ and $r=1$ with 95% C.L., where $\xi = \Gamma(Z^0 \rightarrow h_1^0 h_2^0) / \Gamma(Z^0 \rightarrow \nu_\mu \bar{\nu}_\mu)$ at the Z^0 pole. The dashed curve denotes the prediction of the Glashow-Manohar model.

(c) Excluded region in $M(\tilde{\chi}_2^0) - \tilde{\xi}$ plane with 95% C.L., where $\tilde{\xi} = \Gamma(Z^0 \rightarrow \tilde{\chi}_2^0 \tilde{\chi}_1^0) / \Gamma(Z^0 \rightarrow \nu_\mu \bar{\nu}_\mu)$ at the Z^0 pole. The dashed curve denotes the prediction for maximum higgsino mixing within two doublet models.

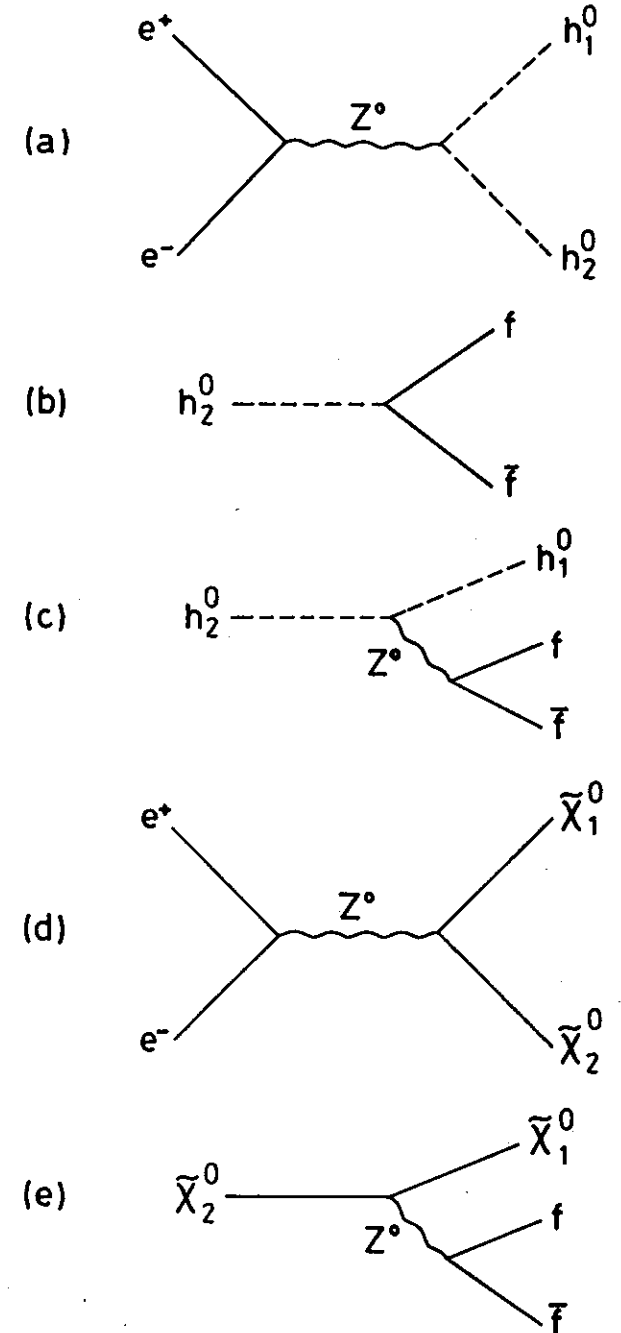


Fig.1

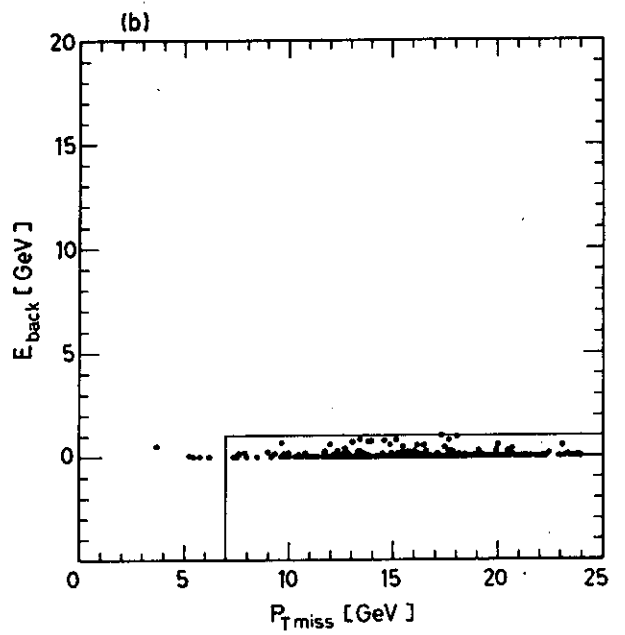
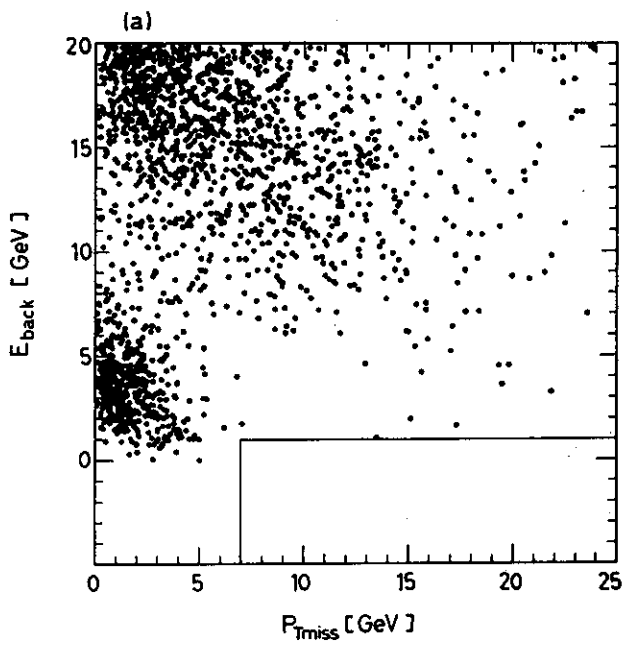


Fig.2

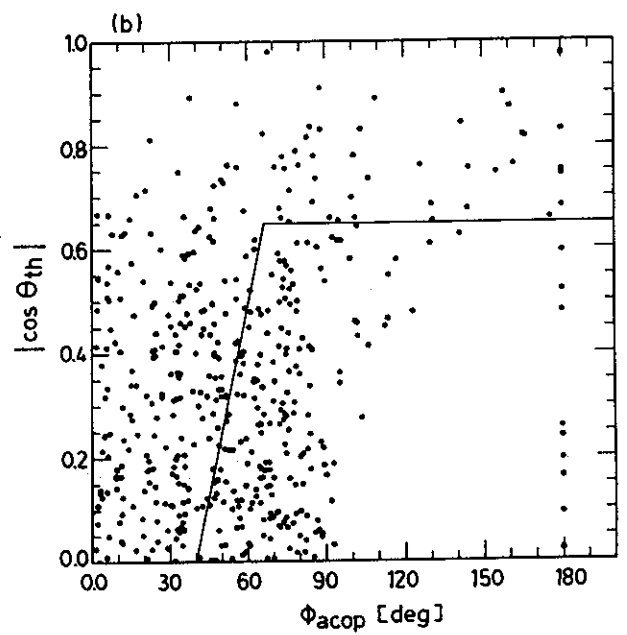
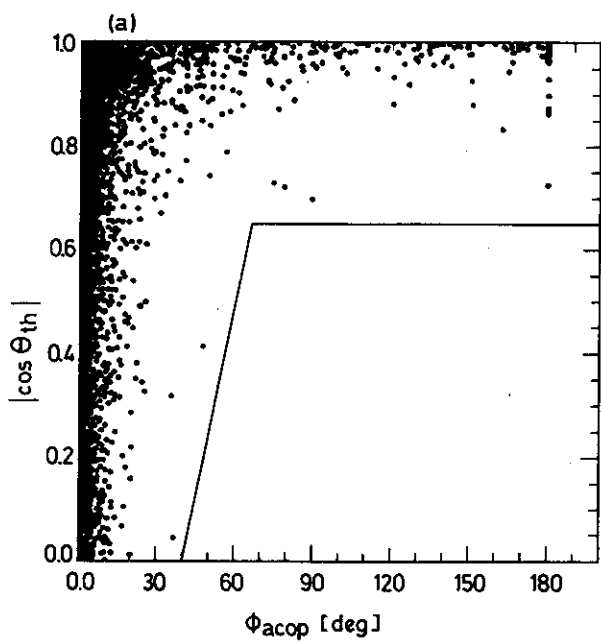


Fig.3

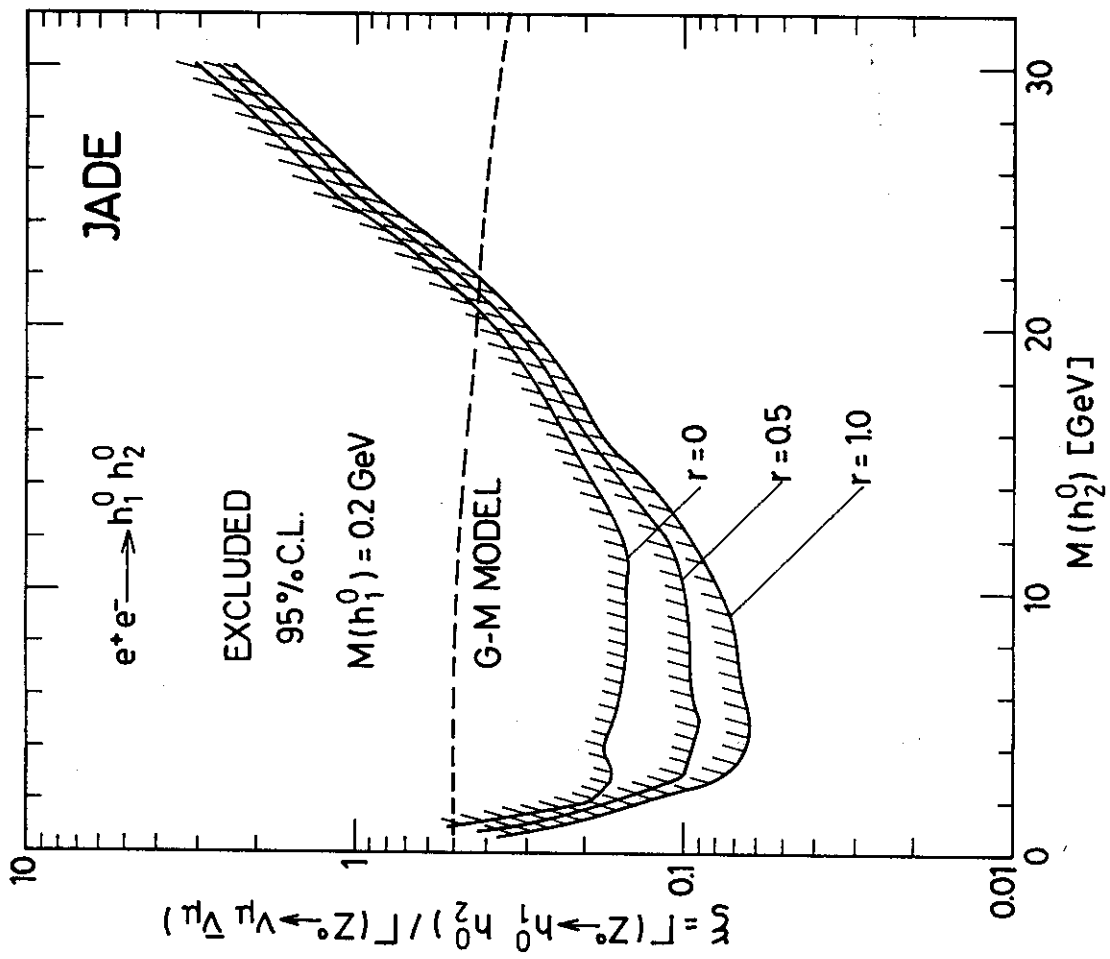


Fig.4(b)

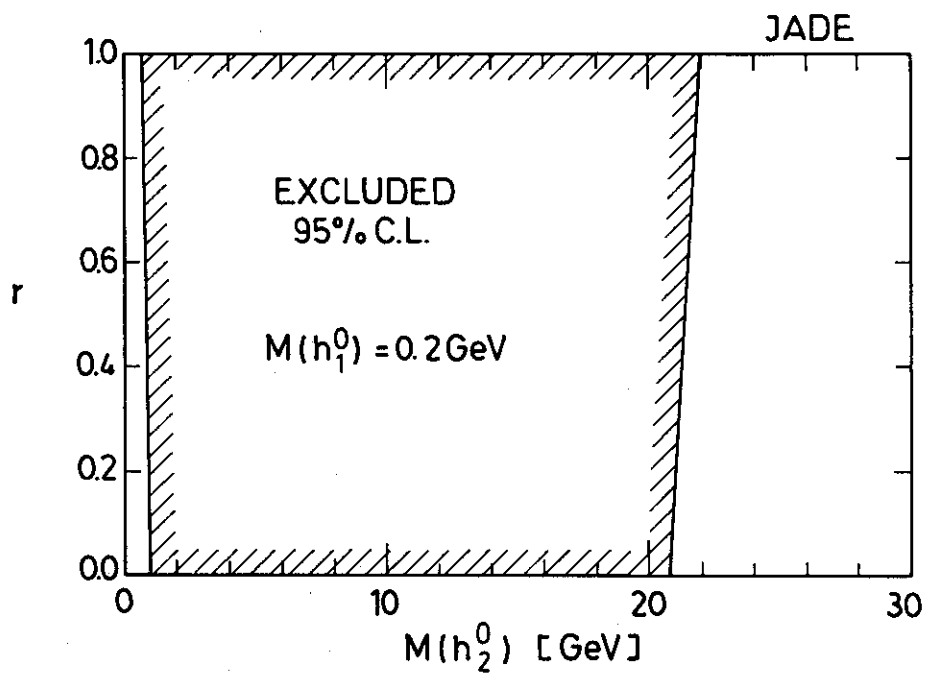


Fig.4(a)

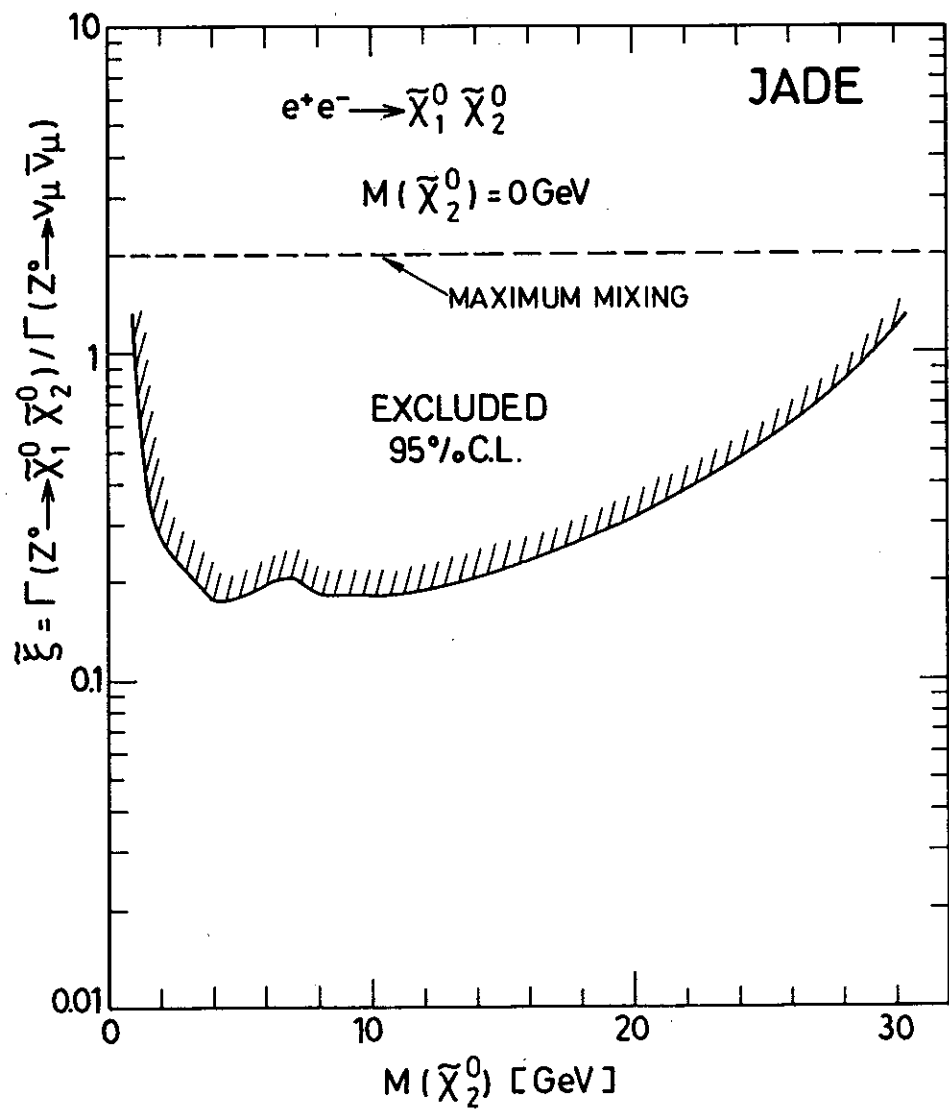


Fig.4(c)